DEVELOPMENT OF FRAGILITY CURVES OF MASONRY BUILDINGS BUILD IN A REGULAR ROW AGGREGATE

M. Demšić[1], S. Pinasco[2], A. Pilipović[1], S. Cattari[2], S. Lagomarsino[2], M. Šavor Novak[1], & M. Uroš[1]

[1] University of Zagreb Faculty of Civil Engineering, 10000 Zagreb, Croatia, marija.demsic@grad.unizg.hr

[2] Department of Civil, Environmental, and Chemical Engineering, University of Genoa, 16145 Genova, Italy

Abstract: *The 2020 earthquakes in Zagreb caused significant structural damage to historic masonry buildings in the city centre although the earthquakes were of moderate magnitude. Typical brick masonry buildings were built in the late 19th and early 20th centuries with three or more stories in height. These buildings are characterised by load-bearing walls dominantly positioned in longitudinal direction that is parallel to the street and wooden beam horizontal structures with a span of approximately 5 to 6 meters. They also have a relatively high interstorey height of around 3.5 to 4 metres. Moreover, such buildings are usually built within city blocks in the form of regular aggregate. A post-earthquake damage revealed that the position of the building within the block as well as differences in height of adjacent buildings has an important role in its behaviour during the earthquake. The topic of this paper is the seismic assessment of a typical historical building in the centre of Zagreb. Fragility curves are developed for the case of a building within the row aggregate by also modelling two adjacent buildings that have a different height than the buildings in question. Non-linear time history analyses are performed on a 3D model in the Tremuri software - which works according to the equivalent frame approach- with the aim of developing fragility curves associated to the in-plane global response. Out-of-plane wall failure mechanisms are also considered, and the fragility curves are developed for this case by referring to the macro-block model strategy. Special attention is paid to the selection of ground motion records for the site. The on-site hazard is calculated using probabilistic seismic hazard assessment while ground motions for each intensity level are selected based on the conditional spectrum. The comparison of fragility curves associated to two damage modes highlighted a higher vulnerability to the out-of-plane response with is consistent with the evidence from the actual observed damage.*

1 Introduction

The activities in Croatia following the two earthquakes in 2020 have shown that the seismic vulnerability of the exposed building stock is a major problem. The first earthquake in March 2020 with a magnitude of 5.3 (Mw) shook the urban area of Zagreb, the intensity was estimated at VII on the EMS-98 scale, the epicentre of the earthquake was located about 7 kilometres northeast of the centre of Zagreb, namely in the Podsljeme district, at a depth of 10 kilometres (Šavor Novak et al. 2020). It is worth noting that the financial losses (Government of Croatia, 2020) caused by this earthquake far exceeded expectations for an event of this magnitude, which was much smaller than expected for the location (Atalić et al. 2018). The fact that the historic centre of Zagreb has a very old building stock with URM buildings having more than three storeys and a considerable number of heritage buildings in the city contributed significantly to this. Nine months later, on December 29, 2020, a strong earthquake of magnitude 6.4 (Mw) and intensity level VIII on the EMS-98 scale occurred in central Croatia, the epicentre of which was only 6 km southwest of the city of Petrinja, about 50 km from Zagreb. This strong earthquake caused extensive damage to buildings, particularly in Petrinja, the nearby towns of Glina and Sisak, and throughout Sisak-Moslavina County and neighbouring counties, including progressive damage to buildings in Zagreb (Atalić et al. 2023).

After the Zagreb and Petrinja earthquakes, efforts were made to improve earthquake-related capacities in order to bolster research capacities in earthquake engineering in Croatia. One of the most important research activities concerns the investigation of residential buildings in the city centre of Zagreb (Pinasco et al. 2023, Moretić et al. 2022, Stepinac et al. 2021). These historic buildings are mainly built within the 'row' aggregates (see Figure 1a), their construction period is followed the Zagreb earthquake of 1880 (Šavor Novak et al. 2020). The aggregates located in the Lower Town of Zagreb are in the area of 3.5 km2, and 72% refers to 168 aggregates while rest of 28% are is part of streets and squares. Most of multi-apartment buildings that have in average 5 storeys occupy 40 to 60% of their plots, and in some cases (for total of 8 aggregates) land utilization is even 80 to 100% (Kiš-Bonačić et al. 2009). Problems contributing to the inadequate seismic design of these buildings include flexible wood beam floors lacking diaphragmatic behaviour, poor material quality (especially mortar), poorly constructed spandrels affecting wall connections, and inadequate connections between load-bearing walls and the floor structure, and uneven stiffness distribution in the vertical elements (Atalić et al. 2021).

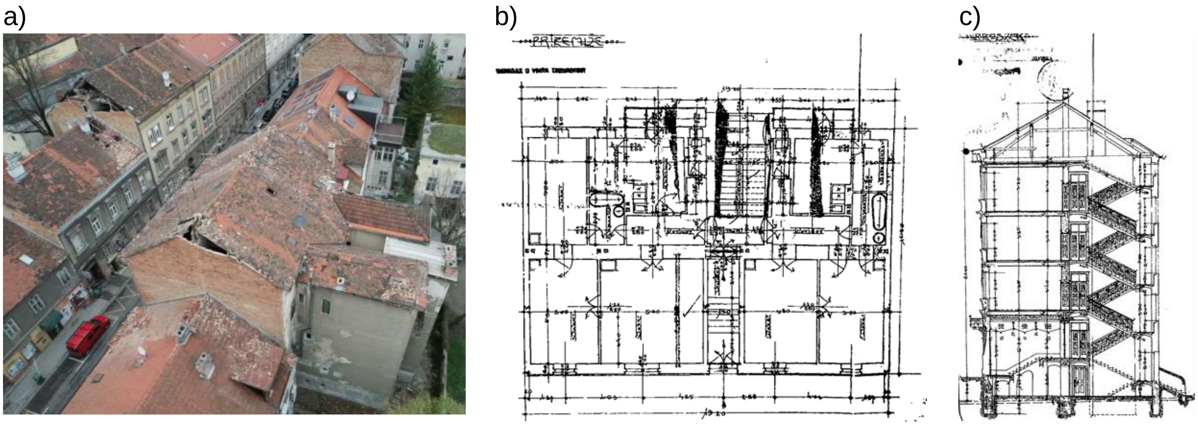

Figure 1 Traditional URM masonry buildings in row aggregate in Zagreb Lower Town (a); Achieve documentation: floor plan and building cross section of typical URM building (b and c).

The preliminary analysis given by the Authors in Pinasco et al. (2023) included a typical URM building (Figure 1 b and c) modelled as free-standing and by two adjacent buildings in row aggregate. In the numerical investigations, the equivalent frame (EF) modelling approach was adopted by using the Tremuri software, taking into account the in-plane response and performing non-linear static analyses and dynamic analyses using the Zagreb and Petrinja earthquake records. The model that included the aggregate effect showed a lower vulnerability than that of the isolated building and generally gave a better description of the actual damage to the building. In addition, it should be noted that buildings that were aligned in a row aggregate during the Zagreb earthquake proved to be more resilient, as minor to moderate damage was observed on these buildings. However, there were some exceptions, e.g. buildings higher than the adjacent buildings proved to be more vulnerable, with significant damage occurring in the 'free-standing" floors above the adjacent buildings.

In the present work, this aggregate model is further developed to account for the influence of different building heights, and nonlinear dynamic analyses are performed to develop fragility curves. When selecting the ground motions for the nonlinear dynamic analyses, special attention is paid to ensure that they are consistent with the seismic hazard on site. Nonlinear time-history analyses (NDA) are performed on a 3D-EF model to obtain in-plane seismic performance of the building. In the study of out-of-plane (OOP) mechanisms, the assumption of a rigid block was used by adopting a three-linear analytical constitutive model proposed in Angiolilli et al. (2021). The seismic input for this analysis was based on floor accelerations obtained by post-processing data from the global 3D model. The fragility curves considering only the in-plane response are compared with those including the out-of-plane response.

2 Ground motion selection for dynamic analyses

Special care is taken in selecting ground motions for nonlinear dynamic analyses to stay consistent with the seismic hazard on location. To minimize the uncertainties in input ground motions the conditional spectrum approach is used (Kohrangi et al. 2017) which conditions the ground motions to a specific conditioning period or period range when selecting appropriate ground motions for each intensity level.

Multiple stripes analysis method is chosen for developing analytical fragility curves (Bazzurro et al. 1998). A total of nine intensity levels are chosen which correspond to return periods T_R=50, 95, 225, 475, 975, 2475, 5000, 10000 and 100000 years. Such high return periods are needed in order to capture the higher damage states of the aggregate (hazard levels for Zagreb are only moderately high). When considering the optimal intensity measure choice for this building type, previous research (Pilipović and Uroš, 2022) suggests using average spectral acceleration ($S_{a,avg}$) in a range of periods, which is adopted here as conditioning intensity measure with period range 0.2s – 0.7s and is calculated in increments of 0.1s, taking the geometrical mean to arrive at the final $S_{a,avg}$ value.

Seismic hazard levels are computed using the OpenQuake engine (Pagani et al. 2014) and the European seismic hazard model of 2020 (ESHM20) (Danciu et al., 2021). A collapsed source model logic tree is used, and mean hazard values are calculated. Both classical probabilistic seismic hazard assessment (PSHA) and disaggregation calculations are performed for a characteristic site in Zagreb city center. The obtained hazard curve is shown in Figure 2 along with disaggregation results (characteristic scenario magnitude, distance from source and ϵ value) for the return period T_R=475 yrs. Chosen intensity levels are evenly spaced between each other on the hazard curve. Disaggregation results show that hazard predominantly comes from a known primary seismic source (Herak et al. 2009).

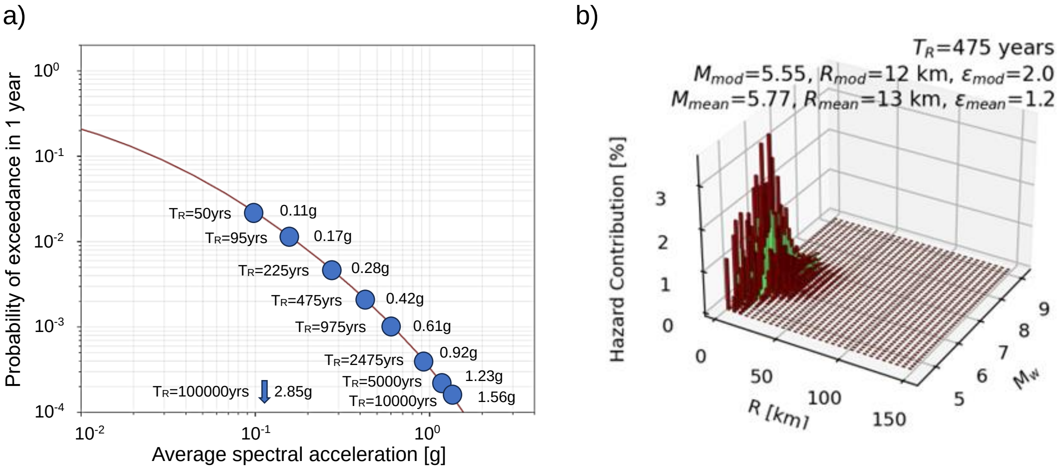

Figure 2 Mean seismic hazard curve obtained from PSHA for $S_{a,avg}$ (a) with hazard values for 9 used intensity levels; Hazard disaggregation results for $S_{a,avg}$ and return period TR=475 yrs (magnitude, Joyner-Boore distance, ϵ value, hazard contribution) (b)

Conditional spectrum is chosen as target spectrum (Baker 2011). Its mean and dispersion are computed using the KothaESHM20 ground motion prediction equation (GMPE), which is the backbone GMPE used in ESHM20, and using values from disaggregation (magnitude, distance and ϵ value). Figure 3 shows the obtained conditional spectrum and its dispersion for return period T_R=475 yrs. It should be noted that when using average spectral acceleration $S_{a,avg}$ the dispersion of the conditional spectrum is only reduced in the selected period range, but does not vanish entirely.

An algorithm proposed by Jayaram et al. (2011) is implemented for selecting ground motion records matching the targets for each intensity level. Three real ground motion databases are chosen as a pool from which ground motions are selected: ESM, Peer NGA West 2 (in part) and GNS (Ancheta et al. (2013), Luzi et al. (2020), Van Houtte et al. (2017)). Constraints in magnitudes, shear wave velocity ($v_{s,30}$) values and scale factors are imposed before selection to account for estimated maximum magnitudes (4 – 7) and soil type ($v_{s,30}$ values 180 – 500 m/s). Scale factors are limited to 0.9 – 1.1 for first six intensity levels and 0.7 – 1.5 for the highest three levels. The proposed algorithm performs Monte Carlo simulations of ground motion spectra that comply with the target (initial set) and picks the best match for each simulated spectrum from the ground motion databases. Then a greedy optimization process is performed which minimizes the sum square errors (SSEs) of chosen ground motions with respect to target dispersion and a final "selected set" is chosen (Figure 3). In this way, 30 ground motion records are chosen per intensity level, making a total of 270 records. It is important to note that the records are chosen with two orthogonal horizontal components only and the target $S_{a,avg}$ for each record corresponds to the RotD50 value of the two horizontal components. The vertical component is neglected. The final set of records used in time history analyses is represented in Figure 4 with respect to magnitudes and distances from source. Spectra of selected records are also shown in Figure 4 for return period T_R=475 yrs.

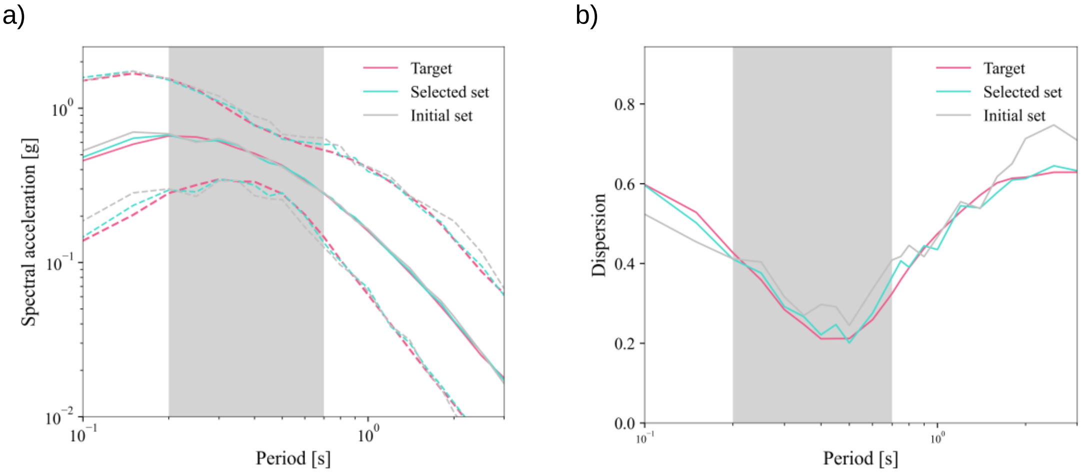

Figure 3 Conditional spectrum with its mean and dispersion for TR=475 yrs. Conditioning spectral acceleration range is highlighted. In this range the dispersion is the lowest. Both the mean initial set and the final mean selected set of ground motion spectra are shown, indicating a good match with the target.

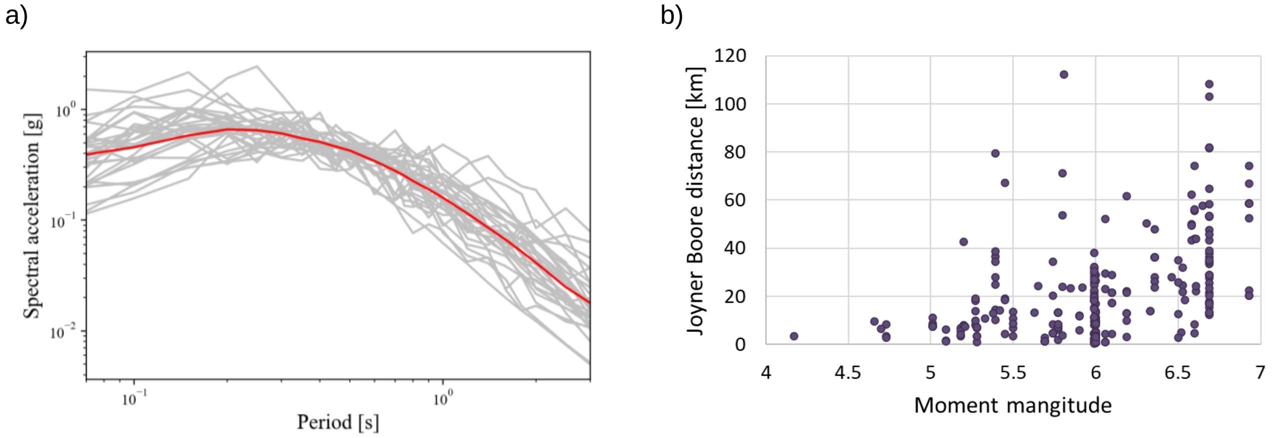

Figure 4 Spectra of selected records and conditional mean spectrum (in red) for return period TR=475 yrs (left); Magnitude – distance relationships of all 270 selected ground motion records (right)

3 Modelling and analysis criteria

3.1 Equivalent frame model for the in-plane response

Figure 5 shows the 3D equivalent frame model of the examined case study. The model was created using Tremuri software (Lagomarsino et al. 2013). A simplified configuration of the model has been already validated in Pinasco et al. (2023) by simulating the actual seismic response of the building within the aggregate following the seismic event that struck the city of Zagreb on March 22, 2020. The EF modelling strategy used refers to nonlinear behaviour concentrated in the masonry panels, namely in the piers (the main vertical structural elements) and spandrels (the horizontal beams connecting piers).

Specifically, the masonry panels are modelled using a nonlinear beam piecewise-linear model proposed in Catari and Lagomarsino 2013. The piecewise-linear beam model (i.e. NLBEAM) has been assumed to describe the nonlinear response of URM panels. This constitutive law allows describing the nonlinear response up to severe damage at the element scale (i.e., DL, from 1 to 5) through progressive strength degradation ($\beta_{E,i}$) corresponding to assigned drift values ($\Theta_{E,i}$) show in Figure 6. The drift thresholds, strength degradation, as well as the parameters governing the hysteretic response, may be differentiated based on the most recurring failure modes characterizing URM panels (i.e., flexural, diagonal cracking shear, or bed-joint sliding) and their type (if piers or spandrels) (Brunelli et al. 2022). The Table 1 reports the strength parameters adopted in the nonlinear dynamic analyses. These parameters, considered deterministic in this research, are consistent with those carried out in various experimental campaigns (Vanin et al. 2017; Kržan et al. 2015), and their reliability in reproducing the seismic response of the Zagreb building has already been verified in Pinasco et al. (2023). Please refer to Cattari et al. (2018) and Angiolilli et al. (2021) for further details on the formulation of NLBEAM and its potential in executing NDA.

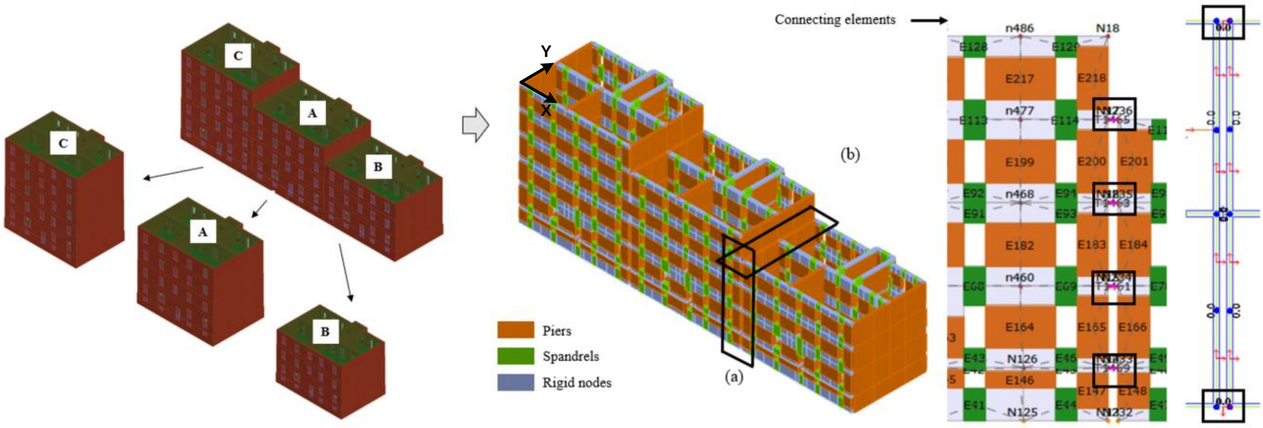

Figure 5 3Muri model of the case study building in both isolated and aggregate configuration; detail of the model elevation at the connection between two adjacent structural units and detail of the elastic truss elements with null tensile behaviour and of the fictious floor connecting two adjacent units

Table 1. Parameters adopted in the non-linear analysis for in-plane response.

	SHEAR								
	dirft Θ [%]			*residual strength β [%]*		*hysteretic response*			
	DL3	DL4	DL5	DL3	DL4	c1	c2	c3	
PIERS	0.47	0.73	0.94	0.6	0.2	0.8	0.8	0	
SPANDRELS	0	1	1.5	0.6	0.6	0.2	0	0.3	
	FLEXURAL								
	dirft Θ [%]			*residual strength β [%]*		*hysteretic response*			
	DL3	DL4	DL5	DL3	DL4	c1	c2	c3	c4
PIERS	0.6	0.9	1.2	1	0.85	0.9	0.8	0.6	0.5
SPANDRELS	0.6	1	1.5	1	0.6	0.2	0	0.3	0.8

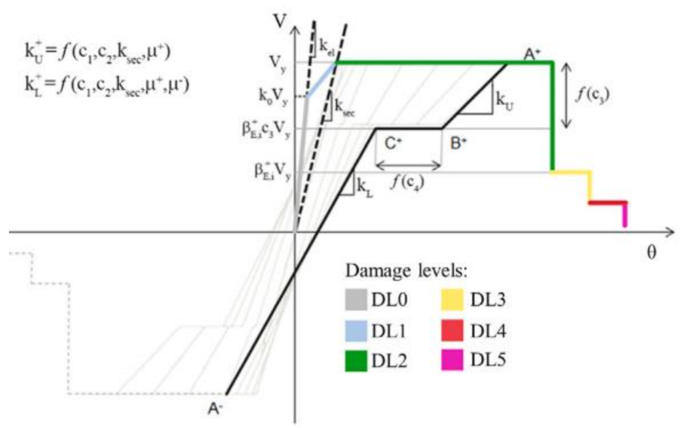

Figure 6 Piecewise-linear constitutive law and hysteretic response of the model

To explicitly account for the interaction effect between adjacent units in the aggregate configuration, the procedure proposed in Angiolilli et al. (2021, 2023) has been implemented. Thus, the units were modelled separately from each other by introducing a finite-length gap representing the semi-length of the shared wall and then connected by elastic truss elements (sectional area of 0.00164 m2 and elastic modulus E of 210,000 MPa with null tensile behaviour) as well as orthotropic membranes (thickness of 0.05 m, E = 39,420 MPa, G = 13,112 MPa) to simulate possible transversal sliding between structural units. Struts, on the other hand, allow modelling the ability of structural units to spread apart while avoiding the interpenetration of elements.

3.2 Modelling out-of-plane response

For the local mechanisms associated with the OOP responses, the walls of building A on the upper floor on both sides of the façades and the gable wall next to building B, which has a lower height than building A under consideration, were taken into account. The one-way cantilever mechanisms are very frequently observed as OOP collapse mechanisms in URM structures in post-earthquake surveys. Furthermore, the walls of the top floor were selected also because of the filtering effect of the building response that tends to be higher on top floors (Degli Abbati et al. 2018) and, in particular, for the attic gable wall since, next to the chimney collapse, it was the most frequent damage observed after the Zagreb earthquake (Šavor Novak et al. 2020). For the façade walls, the three-linear SDOF constitutive model proposed in Angiolilli et al. (2021) was used, which assumes an interlocking effect with perpendicular walls and a simple bi-linear relation for the gable wall. The dynamic equation is given by:

$$\ddot{d}^* + 2\xi\omega_{eq}\dot{d}^* + \omega_{eq}^2 d^* = -a^* \tag{1}$$

where a* is floor accelerations obtained by post-processing data from the global 3D model represented by the response to spatial nodes of the equivalent frame model for the component that is perpendicular to the wall plane, the equivalent viscous damping constant is assumed to be 0.05, and ω_{eq} depends on the displacement of the local mechanism:

$$\omega_{eq}^2 = \begin{cases} \left(2\pi / T_{eq}\right)^2 & d^* \le \gamma_r d_0 \\ \left(\alpha_0 + \alpha_i\right)/d^* - \left(\beta_r\alpha_0 + \alpha_i\right)/\left(\beta_r d_0\right) & \gamma_r d_0 < d^* < \beta_r d_0 \\ \alpha_0 / d^* - \alpha_i / d_0 & d^* \ge \beta_r d_0 \end{cases} \tag{2}$$

The selected walls and the constitutive model, represented in terms of OOP displacement (d*) and pseudo-acceleration (a*), are shown in Figure 7 with the initial points of the panel state described in Table 3. The rigid body motion depends solely on the pseudo-acceleration (α_0) and interlocking contribution (α_i), while a simplified approach is chosen for the equivalent period value T_{eq}, which takes into account that the damage level induced by a higher seismic intensity influences the period value. It is assumed that $T_{eq} = T_{el} \cdot dc^{0.5}$, where T_{el} is the elastic period determined in the 3D model and dc is the ductility coefficient $dc = d_{max}/d_y \ge 1$. The d_0 is ultimate displacement and coefficient γ_r is determined by accounting for first intersection of linear branches of a*, while value 0.6 is used for the coefficient β_r that determines second intersection of branches. The calculation parameters of the local mechanisms are given in Table 2. To associate the attainment of DL to the OOP response, all façade walls were considered equally important as they support the wooden beams of the horizontal structures, while the gable wall is considered to be of lesser structural importance (Table 3).

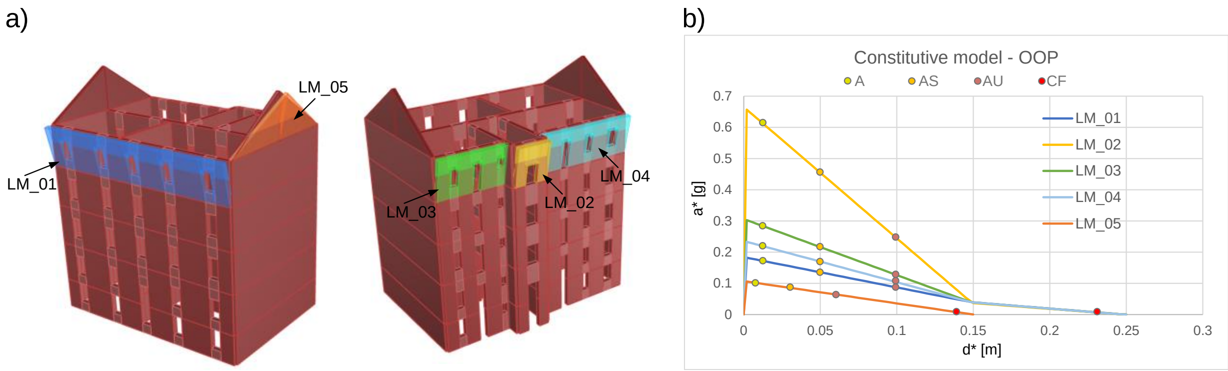

Figure 7 Representation of the walls investigated for the OOP analysis (a); Constitutive model for each depicted local mechanism with the marking of specified states depending on out-of-plane displacement d and pseudo-acceleration a*.*

Table 2. Parameters of the local mechanisms considered: H – panel height; B – panel thickness; P_{roof} – weight transmitted from the roof assumed acting at 2/3 of B; P_{wall} – weight of the wall and t_s – total thickness of orthogonal panels that contribute to interlocking

	H [m]	B [m]	P_{roof} [kN]	P_{wall} [kN]	ts [m]
LM_01	3.85	0.45	245.41	536.43	0.9
LM_02	3.85	0.45	36.95	80.23	0.9
LM_03	3.85	0.45	76.58	174.20	0.7
LM_04	3.85	0.45	115.35	264.18	0.7
LM_05	4.20	0.3	0	146.74	0

Table 3. Definition of states during response of panels in OOP and its contribution to global DL depending on number of panels that had certain limit value of d_{max}.

A = activated $0.05d_0 < d^*_{max} \leq 0.2d_0$
AS = activated with high probability of stable response $0.2d_0 < d^*_{max} \leq 0.4d_0$
AU = activated with high probability of unstable response $0.4d_0 < d^*_{max} \leq 0.95d_0$
CF = certain failure $d_{max} \geq 0.95d_0$

DL0	DL1	DL2	DL3	DL4	DL5
NO = 4	A ≥ 1 or A/AS of gable	AS ≥ 1 or AU of gable	1 ≤ AU ≤ 3 or CF of gable	AU = 4 or 1 ≤ CF ≤ 3	CF = 4

4 Results of dynamic performance assessment and fragility curves

The case study was first investigated by modal analyses on both the entire 3D EF model of the aggregate (i.e. from unit A to unit C) and the ones developed for the individual structural units to obtain a preliminary insight into their dynamic behaviour. The values of the structure's periods reported in Table 4 refer to the transverse direction (Y direction in Figure 5).

Table 4. Fundamental periods of units and of aggregate.

	Unit A	Unit B	Unit C	Aggregate
Period (s)	0.333	0.253	0.421	0.413

Figure 8 shows the capacity curve of central unit A, considered within the aggregate, compared with that of the entire aggregate for both the longitudinal (X) and transverse (Y) directions. The curves are expressed in terms of base shear versus roof drift and have been obtained through NSA by applying a uniform force distribution proportional to the mass in X and Y direction and both verses.

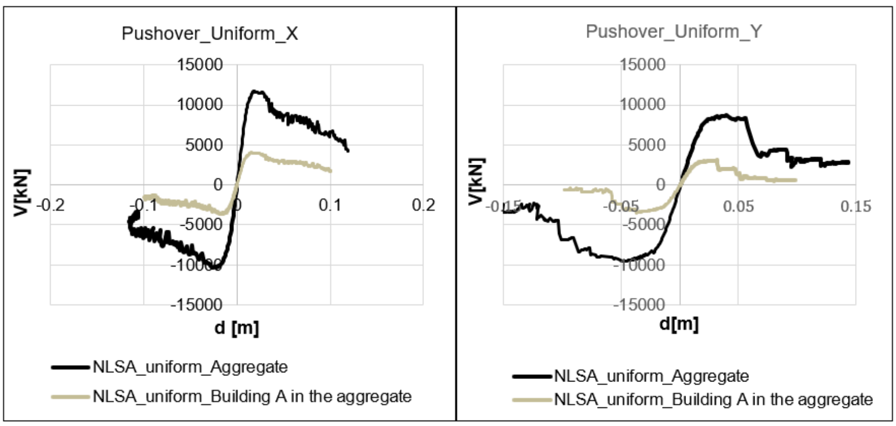

Figure 8 Pushover curves of central unit A, considered within the aggregate, compared with that of the entire aggregate for both the x and y directions

Figure 9 shows time-history response obtained by NDA for the façade wall LM_01 for two different intensity levels, indicating that different input floor accelerograms (three nodes are considered for LM_01) can lead to different states of a local mechanism under consideration. For the final estimation, the most unfavourable input floor acceleration case of the three-node response is chosen for the definition of the OOP limit state.

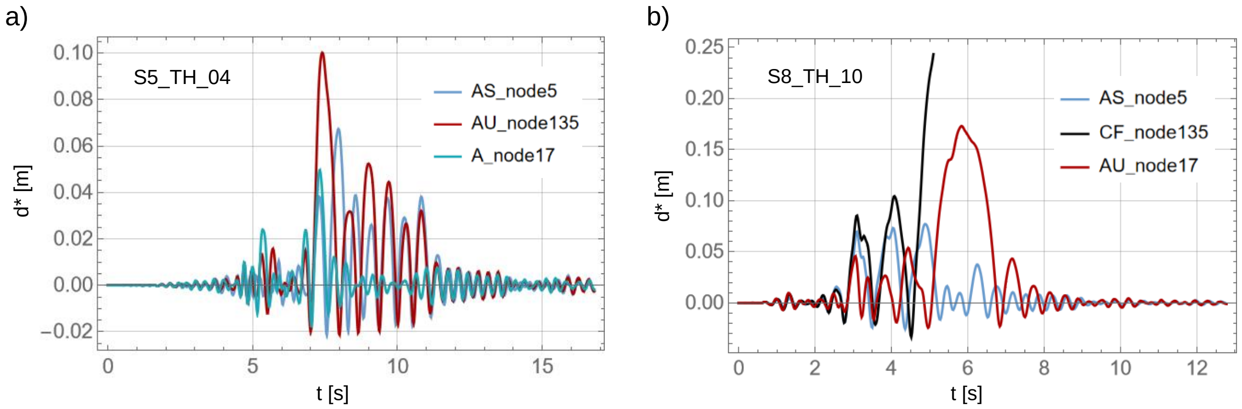

Figure 9 Time-history response function of d for LM_01 during a specific NDA case*

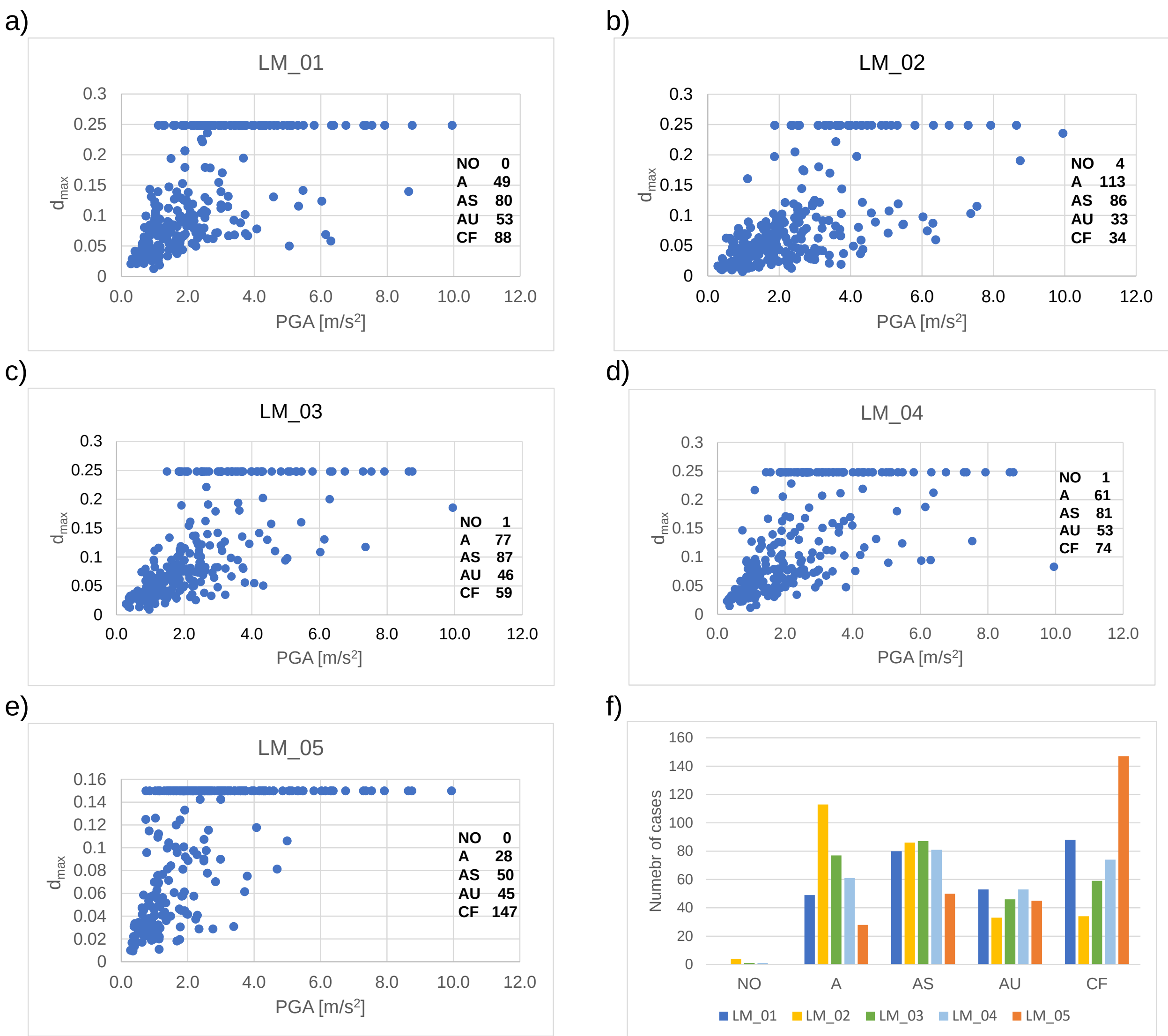

Figure 10 Maximum displacement of local mechanisms obtained by the time-history analysis (a-e) and histogram of achieved response state for each (f).

Figure 10 shows the results in terms of the maximum OOP displacement obtained by the NDAs of the investigated local mechanisms. It can be observed that the value of d_{max} tends to increase when the PGA value is higher. Moreover, analysing the number of fulfilled states of OOP considering stability is consistent with the contribution of interlocking, which can also be seen in Figure 7b. It is worth noting that all façade walls (LM_01-LM_04) have the same thickness and some minor differences in the centre of gravity (x_G, z_G). Therefore, it is consequential that the results show that LM_01 has a higher probability of unstable response (AU and CF) than, for example, LM_02, where the effect of interlocking is greater. Apart from this, it is also interesting to observe the very low number of NO activations of local mechanisms (here only 4 cases for LM_02 and 1 for LM_03 and LM_04), which can be correlated with the building height. As already mentioned, the higher floors have a more pronounced filtering effect, i.e., the floor accelerations tend to increase on the upper levels of the building. Finally, when considering attic gable wall (LM_05), CF can be expected in more than half of the cases.
Within the aim of deriving fragility curves, it is necessary to synthetically interpret the structural response data derived from the NLDAs. To assign a specific damage level to the building compatible with the EMS98 scale (i.e., from DL1 to DL5), i.e., to determine the overall building damage level (Table 5), the damage reached at the “wall scale” was analysed similarly to what was done in Angiolilli et al. (2021, 2023) and for the out-of-plane response proposed damage levels are given in Table 3. The derivation of the fragility curves was performed by the R2R software adopting the least squares fit Baraschino et al. (2020) and Iervolino (2017) assigning damage levels reached in a frequentist manner given in Figure 11.

Table 5. Overall building damage level.

		Sa(T1)	DL0		DL1		DL2		DL3		DL4		DL5	
			IP	OOP	IP	OOP	IP	OOP	IP	OOP	IP	OOP	IP	OOP
S1	**Tr = 50 years**	**0.11**	**0**	**27**	**18**	**3**	**11**	**0**	**1**	**0**	**0**	**0**	**0**	**0**
S2	**Tr = 95 years**	**0.17**	**0**	**20**	**16**	**10**	**8**	**0**	**6**	**0**	**0**	**0**	**0**	**0**
S3	**Tr = 225 years**	**0.28**	**0**	**7**	**2**	**21**	**17**	**2**	**7**	**0**	**4**	**0**	**0**	**0**
S4	**Tr = 475 years**	**0.42**	**0**	**1**	**0**	**21**	**9**	**8**	**15**	**0**	**6**	**0**	**0**	**0**
S5	**Tr = 975 years**	**0.59**	**0**	**0**	**0**	**20**	**5**	**8**	**15**	**0**	**10**	**1**	**0**	**1**
S6	**Tr = 2475 years**	**0.89**	**0**	**0**	**0**	**6**	**1**	**22**	**12**	**0**	**15**	**1**	**2**	**1**
S7	**Tr = 5000 years**	**1.23**	**0**	**0**	**0**	**3**	**0**	**24**	**9**	**1**	**21**	**2**	**0**	**0**
S8	**Tr = 10000 years**	**1.56**	**0**	**0**	**0**	**1**	**0**	**20**	**5**	**4**	**21**	**4**	**4**	**1**
S9	**Tr = 100000 years**	**2.85**	**0**	**0**	**0**	**0**	**0**	**7**	**2**	**6**	**16**	**6**	**12**	**11**
TOTAL			**0**	**55**	**36**	**85**	**51**	**91**	**72**	**11**	**93**	**14**	**18**	**14**

Fragility curves for in-plane and out-of-plane are shown on Figure 10. It can be seen from the fragility curves that the probability of damage due to out-of-plane mechanisms is much more frequent and more likely than in-plane damage mechanisms. For the same value of the intensity measure, the probability of in-plane damage is much lower than out-of-plane. Moreover, out-of-plane failure mechanisms are dominant and represent the primary problem for moderate earthquakes for such building type.
In order to compare the results with actual damage during the 2020 Zagreb earthquake, the pseudo-acceleration value for the dominant natural period of the structure is marked. For this value of pseudo-acceleration, it can be noted that mostly light damage to the vertical structure is to be expected, while out-of-plane mechanisms have moderate damage with a certain probability of collapse. Such a condition corresponds to the actual damage that was documented in Šavor Novak et al. (2020), Atalić et al. (2020), Stepinac et al. (2021), where the dominant damage was the overturning of gable walls, chimneys and unsupported attic walls. Figure 12 shows typical damage to a block in Zagreb after the 2020 earthquake. For stronger earthquakes, this problem is even more pronounced. For the expected earthquake with a return period of 475 years for which S_a=0.74g, moderate damage to the vertical structure can be expected, as well as the failure of most of the unsupported walls of the attic.

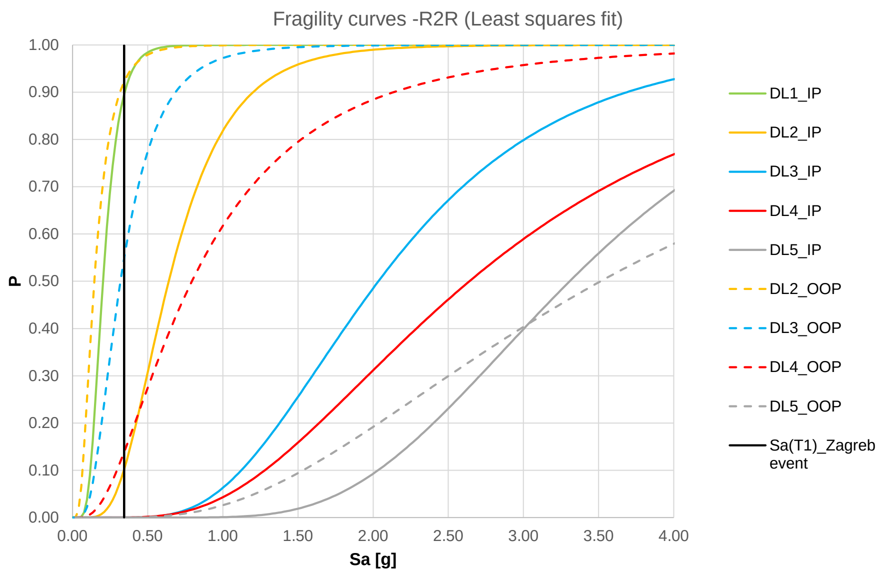

Figure 11 Fragility curves considering global in-plane and out-of-plane response

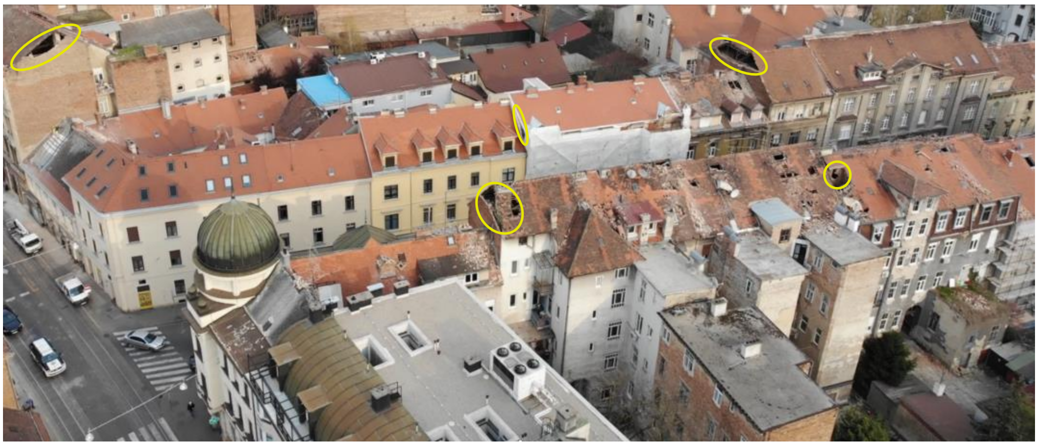

Figure 12 Damage to a typical building block in Zagreb after the 2020 earthquake.

5 Conclusions

The study herein presented aimed at providing an evaluation of both the in-plane and out-of-plane seismic response of an existing unreinforced masonry row aggregate located in the historic centre of Zagreb Lower Town. Particular attention is paid to the selection of ground motion records for the non-linear dynamic analyses to adapt them to the local seismic hazard. For assessing the in-plane seismic performance by NDAs, a 3D-equivalent frame model which explicitly considers the interaction effects between the structural units has been used,. In addition, the top floor accelerations obtained from the global response by post-processing are used as seismic input to evaluate the local OOP mechanisms. For each damage mode, the fragility curves were generated using the R2R software, employing the least squares fit method.

The results of the fragility curves are consistent with the main evidence from the damage patterns observed after the Zagreb earthquake and the extent of damage in Zagreb Lower Town (Šavor Novak et al. 2020, Atalić et al. 2021, Stepinac et al. 2021), This is particularly true for DL1 - DL2 for global in-plane response and DL2 - DL3 associated to the local out-of-plane responses. However, the DL4-OOP curve, which includes a probability of unstable response or certain collapse of façade walls, appears to give slightly conservative results and a refined model of the local mechanism (altering the configuration of the predetermined geometry or by taking into account influence of additional constraints) or a modification of the DL criteria needs to be considered. To this end, future work will include a more accurate calibration of the results with the actual observed damage to this type of building as a result of the 22 March 2020 Zagreb earthquake.

6 Acknowledgments

The study presented in the article was developed within the research activities of the ReLUIS-DPC 2022-2024 research programs (WP4 and WP10), funded by the Department of Civil Protection and project UIP-2020-02-1128 - New vulnerability models of typical buildings in urban areas: Applications to seismic risk assessment and target retrofitting methodology (2BESAFE) funded by the Croatian Science Foundation.

7 References

Ancheta, T. D., Darragh, R. B., Stewart, J. P., Seyhan, E., Silva, W. J., Brian, A., Chiou, S. J., Wooddell, K. E., Graves, R. W., Kottke, A. R., Boore, D. M., Kishida, T., & Donahue, J. L. (2013). *PEER NGA-West2 Database*.

Angiolilli M., Lagomarsino S., Cattari S., Degli Abbati S. (2021). Seismic fragility assessment of existing masonry buildings in aggregate, *Eng Struct*, vol. 247, p. 113218, doi: 10.1016/J.ENGSTRUCT. 2021.113218.

Angiolilli M., Brunelli A., Cattari S. (2023). Fragility curves of masonry buildings in aggregate accounting for local mechanisms and site effects, *Bulletin of Earthquake Engineering*, pp. 1–43, doi: 10.1007/S10518-023-01635-9/TABLES/8.

Atalić J., Demšić M., Baniček M., Uroš M., Dasović I., Prevolnik S., Kadić A., Šavor Novak M., Nastev M. (2023). The December 2020 magnitude (Mw) 6.4 Petrinja earthquake, Croatia: seismological aspects, emergency response and impacts. *Bulletin of Earthquake Engineering* 21, 5767–5808. https://doi.org/10.1007/s10518-023-01758-z

Atalić J., Uroš M., Šavor Novak M., Demšić M., Nastev M. (2021). The Mw5.4 Zagreb (Croatia) earthquake of March 22, 2020 impacts and response. *Bulletin of Earthquake Engineering* 19(9):3461–3489. https://doi.org/10.1007/s10518-021-011:17-w

Atalić J., Šavor Novak M., Uroš M. (2018). Updated risk assessment of natural disasters in Republic of Croatia—seismic risk assessment (in Croatian), Faculty of Civil Engineering in collaboration with Ministry of Construction and Physical Planning and National Protection and Rescue Directorate, Zagreb, Croatia.

Baker, J. W. (2011). Conditional Mean Spectrum: Tool for Ground-Motion Selection. *Journal of Structural Engineering*, *137*(3), 322–331. https://doi.org/10.1061/(asce)st.1943-541x.0000215

Baraschino R., Baltzopoulos G., Iervolino I. (2020). R2R-EU: Software for fragility fitting and evaluation of estimation uncertainty in seismic risk analysis, *Soil Dynamics and Earthquake Engineering*, vol. 132, p. 106093, doi: 10.1016/J.SOILDYN.2020.106093.

Bazzurro, P., Cornell, A., Member, Z., Asce, N., Shome, /, & Carballo, J. E. (1998). THREE PROPOSALS FOR CHARACTERIZING MDOF NONLINEAR SEISMIC RESPONSE. *Journal of Structural Engineering*, 1281–1289.

Brunelli A., de Silva F., Cattari S. (2021). Site effects and soil-foundation-structure interaction: derivation of fragility curves and comparison with Codes-conforming approaches for a masonry school, *Soil Dynamics and Earthquake Engineering*, vol. 154, no. June 2021, p. 107125, 2022, doi: 10.1016/j.soildyn.2021.107125.

Cattari S., Camilletti D., Lagomarsino S., Bracchi S., Rota M., Penna A. (2018). Masonry Italian Code-Conforming Buildings. Part 2: Nonlinear Modelling and Time-History Analysis, *Journal of Earthquake Engineering*, vol. 22, no. sup2, pp. 2010–2040, doi: 10.1080/13632469.2018.1541030.

Cattari S., Lagomarsino S. (2013). *Masonry structures*, pp. 151-200. In: Sullivan T, Calvi GM, editors. Developments in the field of displacement based seismic assessment. IUSS Press (PV) and EUCENTRE, pp. 524, 2013a. ISBN:978-88-6198-090-7

Danciu, L., Nandan, S., Reyes, C., Basili, R., Weatherill, G., Beauval, C., Rovida, A., Vilanova, S., Sesetyan, K., Bard, P.-Y., Cotton, F., Wiemer, S., & Giardini, D. (2021). *The 2020 update of the European Seismic Hazard Model-ESHM20: Model Overview*.

Degli Abbati S., Cattari S., Lagomarsino S. (2018). Theoretically-based and practice-oriented formulations for the floor spectra evaluation. *Earthquakes and Struct* 15(5): 565–581.

Government of Croatia (2020): Croatia earthquake: Rapid damage and needs assessment, June 2020.

Herak, D., Herak, M., & Tomljenović, B. (2009). Seismicity and earthquake focal mechanisms in North-Western Croatia. *Tectonophysics*, *465*(1–4), 212–220. https://doi.org/10.1016/j.tecto.2008.12.005

Iervolino I. (2017). Assessing uncertainty in estimation of seismic response for PBEE, *Earthq Eng Struct Dyn*, vol. 46, no. 10, pp. 1711–1723, doi: 10.1002/EQE.2883.

Jayaram, N., Lin, T., & Baker, J. W. (2011). A Computationally efficient ground-motion selection algorithm for matching a target response spectrum mean and variance. *Earthquake Spectra*, *27*(3), 797–815. https://doi.org/10.1193/1.3608002

Kiš-Bonačić K., Žic D., Bubrić M. (2009): Zagreb Lower Town: city blocks, catalogue, Institute for Spatial Planning of the City of Zagreb, Croatia

Kohrangi, M., Bazzurro, P., Vamvatsikos, D., & Spillatura, A. (2017). CS based GMR selection using Sa,avg. *Earthquake Engineering & Structural Dynamics*, *46*, 1667–1685.

Kržan M., Gostič S., Cattari S., Bosiljkov V. (2015). Acquiring reference parameters of masonry for the structural performance analysis of historical buildings, *Bulletin of Earthquake Engineering*, vol. 13, no. 1, pp. 203–236, doi: 10.1007/S10518-014-9686-X.

Lagomarsino S., Penna A., Galasco A., Cattari S. (2013). TREMURI program: An equivalent frame model for the nonlinear seismic analysis of masonry buildings, *Eng Struct*, 56: 1787-1799. doi: 10.1016/j.engstruct.2013.08.002.

Luzi, L., Lanzano, G., Felicetta, C., D'Amico, M. C., Russo, E., Sgobba, S., Pacor, F., & ORFEUS Working group 5. (2020). *Engineering Strong Motion Database (ESM) (Version 2.0)*.

Moretić A., Chieffo N., Stepinac M., Lourençο P. B. (2022). Vulnerability assessment of historical building aggregates in Zagreb: implementation of a macroseismic approach, *Bulletin of Earthquake Engineering*, no. 0123456789, 2022, doi: 10.1007/s10518-022-01596-5

Pagani, M., Monelli, D., Weatherill, G., Danciu, L., Crowley, H., Silva, V., Henshaw, P., Butler, L., Nastasi, M., Panzeri, L., Simionato, M., & Viganò, D. (2014). OpenQuake Engine: An Open Hazard (and Risk) Software for the Global Earthquake Model. *Seismological Research Letters*, *85*, 692–702. https://doi.org/10.1785/0220130087

Pilipović A., Uroš, M. (2022). Selection of optimal intensity measure for a typical masonry building in the urban area of Zagreb. In Štirmer Nina (Ed.), *8th Doctoral symposium in Civil Engineering* (pp. 111–124). University of Zagreb (in Croatian)

Pinasco S., Cattari S., Lagomarsino A., Demšić M., Šavor Novak M., Uroš M. (2023). Numerical investigation of the seismic response of an unreinforced masonry residential buildings hit by Zagreb earthquake in 2020, *Proceedings of the 2nd Croatian Conference on Earthquake Engineering*, Zagreb, Croatia. doi: https://doi.org/10.5592/CO/2CroCEE.2023.125

Stepinac M., Lourenco P.B., Atalić J., Kišiček T., Uroš M., Baniček M., Šavor Novak M. (2021). Damage classification of residential buildings in historical downtown after the ML5.5 earthquake in Zagreb, Croatia in 2020, *International Journal of Disaster Risk Reduction*, vol. 56, no. February, 2021, doi: 10.1016/j.ijdrr.2021.102140

Šavor Novak M., Uroš M., Atalić J., Herak M., Demšić M., Baniček M., Lazarević D., Bijelić N., Crnogorac M., Todorić M. (2020). Zagreb earthquake of 22 March 2020—preliminary report on seismologic aspects and damage to buildings. *J Croatian Assoc Civil Eng* 72(10):843–867

Van Houtte, C., Bannister, S., Holden, C., Bourguignon, S., & McVerry, G. (2017). The New Zealand Strong Motion Database. *Bulletin of the New Zealand Society for Earthquake Engineering*, *50*(1), 1–20. https://doi.org/10.5459/bnzsee.50.1.1-20

Vanin F., Zaganelli D., Penna A., Beyer K. (2017). Estimates for the stiffness, strength and drift capacity of stone masonry walls based on 123 quasi-static cyclic tests reported in the literature, *Bulletin of Earthquake Engineering*, 15(12), pp. 5435–5479, doi: 10.1007/S10518-017-0188-5/TABLES/15.